Excitation of bright and dark envelope solitons for magnetostatic waves with attractive nonlinearity

Mark M. Scott,[1] Mikhail P. Kostylev,[2] Boris A. Kalinikos,[2] and Carl E. Patton[1]

[1]*Department of Physics, Colorado State University, Fort Collins, Colorado 80523, USA*
[2]*St. Petersburg Electrotechnical University, 197376 St. Petersburg, Russia*
(Received 3 September 2004; published 31 May 2005)

Dark and bright envelope solitons have been generated from a single magnetostatic carrier wave with attractive nonlinearity. The solitons were formed through the mode beating of two microwave input signals with frequency separations of 3–30 MHz for an in-plane magnetized single crystal yttrium-iron-garnet film in the magnetostatic backward volume wave configuration. Numerical modeling based on the Ginzburg-Landau equation model gave good agreement with the data.

Two different types of envelope solitons, bright and dark, can propagate in nonlinear dispersive media. The description of these envelope solitons is typically given by the cubic one-dimensional nonlinear Schrödinger (NLS) equation. The key factors, which determine the solutions of the NLS equation, are the dispersion D and nonlinear N coefficients. Physically these two coefficients represent the curvature of the frequency versus wave number dispersion and the change in the carrier frequency with signal amplitude, respectively. It is convenient to use these factors to characterize wave propagation in nonlinear dispersive waveguiding media. When the sign of the product of the dispersion parameter D and nonlinear parameter N is opposite, one has attractive nonlinearity, which describes media where bright soliton formation is possible. When the sign of this product is positive, one has repulsive nonlinearity, which describes media where dark soliton formation is possible (see, e.g., Refs. 1 and 2). In the situations that could be theoretically treated in the frames of the nonlinear Schrödinger (NLS) equation model, the formation of bright and dark solitons under these conditions is well established. Examples include deep water, plasmas, optical fibers, electrical transmission lines, and magnetic films.[2–4] Some of the evident demonstrations have been for magnetostatic wave solitons in magnetic films.[5–11] A theoretical treatment of magnetostatic wave soliton formation in magnetic films leading to the NLS equation model and consequently to the existence of both bright and black envelope solitons was given in Ref. 12.

This paper reports the experimental generation of two different envelope solitons trains for a single carrier wave propagating in a magnetic medium with attractive nonlinearity. The soliton trains are generated through the nonlinear mode beating of two copropagating magnetostatic backward volume wave (MSBVW) excitations in a thin yttrium–iron–garnet (YIG) film. Furthermore, a theoretical model based on the Ginzburg-Landau equation is presented to explain the observed phenomena.

These results contrast significantly with previous microwave magnetic envelope (MME) soliton work as cited above. In those works, it was possible to explain the experimentally obtained results by applying the NLS equation model. In other words, the sign of the product DN was always a key factor in the excitation of bright or dark solitons. When the condition, $DN<0$, was satisfied, one obtained bright solitons. For the condition $DN>0$, one always obtained dark solitons.

The present realization of MSBVW dark solitons for $DN<0$ was obtained with two balanced equal amplitude copropagating high power cw input signals. Unbalanced input signals give the expected bright solitons. These results show that, dependent only on the amplitude of the input signals, one can have bright or dark solitons for a single carrier wave configuration and a given sign of the DN product. Numerical modeling based on the Ginzburg-Landau equation gives good agreement with the data. This theoretical confirmation indicates that the response is closely related to spin wave nonlinear damping, which is due to decay instability processes.

The experiments utilized a long and narrow 6.9 μm thick single crystal YIG film strip in a MSBVW transducer structure. The low loss liquid phase epitaxy film had unpinned surface spins. A 50 μm wide input microstrip antenna was used for excitation. The cw microwave input signals were obtained from synchronized stable frequency sources. A movable output antenna in the form of a small 200 μm diam inductive loop[13] was used to measure the signal level in the strip as a function of distance from the input antenna. These signals were analyzed in the time and frequency domains with a fast oscilloscope and a microwave spectrum analyzer, respectively.

The YIG film was magnetized in-plane by an applied field H along the long edge of the film and the propagation direction. The choice of frequency and wave number operating points was based on low power measurements of the MSBVW frequency ω_k as a function of wave number k. These $\omega_k(k)$ dispersion data were obtained with a single cw frequency applied to two microstrip lines at opposite ends of the YIG film. For a given ω_k value, the standing wave MSBVW interference response profile along the film was measured with the movable probe to obtain the wavelength λ and wave number $k=2\pi/\lambda$. These data also yielded the MSBVW band edge frequency at zero k, taken as ω_B, and the group velocity $\nu_g=\partial\omega_k/\partial k$ as a function of ω_k and k. A nominal H value of 1310 Oe was used to set the band edge at $f_B=\omega_B/2\pi=5690$ MHz.

For the soliton experiments, the two input frequencies were varied over the low k region of the $\omega_k(k)$ dispersion curve, with input power levels up to 25 dBm. The MSBVW signals were measured at distances from approximately $4-8$ mm from the input. Input cw powers above about 18 dBm were needed to produce a pronounced instability response. Results similar to those shown below could be obtained for f_1 and f_2 frequency values from about 5597 to 5567 MHz, and corresponding nominal wave number values from 100 to 200 rad/cm. The separation frequency, $\Delta f = |f_1 - f_2|$, where f_2 was varied, ranged from 3 to 30 MHz. For Δf values below about 3 MHz, the output signals became severely distorted. For Δf values above 30 MHz, there was no multiharmonic instability response for the available input powers.

The interference between the copropagating MSBVW signals at f_1 and f_2 gave the expected harmonic response at low power and a nonlinear response at high power. The form of the nonlinear response was found to depend critically on the relative values of the two input power levels. When the two powers were unequal, the nonlinear response was in the form of cnoidal waves or bright soliton trains. When the two powers were balanced, the nonlinear response was in the form of dark soliton trains.

This bright/dark changeover is the key result of this report. Heretofore, and as noted above, the MSBVW configuration and the corresponding attractive nonlinearity have been used to produce only bright solitons or bright soliton trains. From the standard notion based on the nonlinear Schrödinger equation model, one would expect to see only bright solitons for the magnetization waves with an attractive nonlinearity. The present data, however, clearly show that one can generate dark solitons for this configuration. Therefore, in the course of these experiments, it became clear that another theoretical model should be used to explain the observed phenomena.

Figure 1 shows representative results on the transition from bright to dark soliton trains that is obtained due to relative changes in the two input power levels P_1 and P_2. For all of the traces shown, f_1 and f_2 were set to 5590 and 5595 MHz, respectively, with corresponding low power MSBVW k_1 and k_2 values of 180 and 170 rad/cm, respectively. The probe position was 5 mm from the input transducer. The solid curves in the left and right side graphs show the detected voltage amplitude (A) versus time and power versus frequency profiles, respectively, for different P_1 and P_2 combinations. All time profiles are scaled to the maximum amplitude. The frequency profiles are shown with uncalibrated decibel scales. The dashed curve in (c-i) shows a phase (P) profile as well. Graphs (a-i) and (a-ii) correspond to $P_1 = 19$ dBm and $P_2 = 25$ dBm and an input power ratio of 1:4. Graphs (c-i) and (c-ii) are for equal input powers at $P_1 = P_2 = 19$ dBm. Graphs (b-i) and (b-ii) are for an intermediate case at $P_1 = 19$ dBm and $P_2 = 24$ dBm.

The time traces in Fig. 1 show the key result, namely, the evolution from a train of bright solitons in (a-i) for unequal cw input powers to a train of dark solitons in (c-i) when the two cw input powers are equal. The train of bright pulses in (a-i) appears against a substantial background. Higher powers than those available here would be expected to reduce
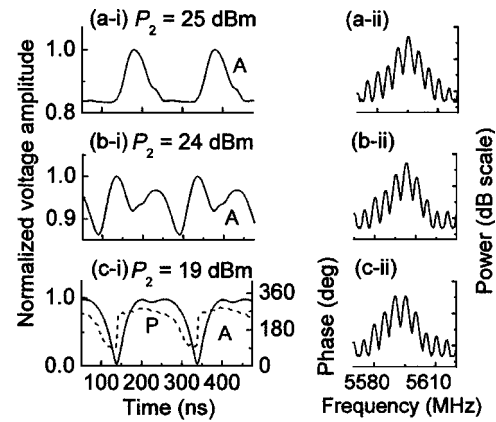

FIG. 1. Normalized voltage amplitude (A) versus time traces and corresponding power versus frequency profiles for a probe detection point 5 mm from the input transducer, with two cw input signals at frequencies $f_1 = 5590$ MHz and $f_2 = 5595$ MHz. The power scales in (a-ii), (b-ii), and (c-ii) correspond to the right hand vertical axes. The input power P_1 was 19 dBm for all traces. The P_2 input powers were as indicated for each set of graphs. Graph (c-i) also shows a phase (P) vs time profile.

this background and give a further steepening and narrowing of the pulses. The train of dips in (c-i) corresponds to the type of profile expected for dark solitons. The fact that the dips in (c-i) are sharp and go essentially to zero voltage means that these are black solitons. This black soliton character is further supported by the phase profile in (c-i). The dashed curve here shows a clear and distinct 180° jump in the phase at the cusp points in the amplitude profile. This is a well-established signature for a black soliton.[2]

The power versus frequency profiles in (a-ii)–(c-ii) provide further insight into the effect of the input signal makeup on the soliton response. When P_2 is 6 dB greater than P_1, as in (a), the dominant peak in the power spectrum is at f_2 and the temporal response is in the form of a cnoidal wave or bright soliton train. The key here is in the unbalanced high power cw input signals. In contrast, when the input powers are equal, as in (c), the power spectrum shows two main peaks with equal amplitudes and the temporal response is in the form of a dark soliton train. The data show that this particular combination of powers and frequencies gives black solitons, a specific subclass of dark soliton as discussed above. The key here is in the balanced high power input signals.

A simple explanation for the formation of dark solitons for magnetostatic spin waves with attractive nonlinearity is given here, based on the fact that the soliton trains are derived from cw excitation and mode beating rather that the pulse inputs used for most of the previous MME soliton experiments. In the cw mode beating process, parametric spin wave interactions with large wave-number transfer are possible.[14] These scattering processes, where a low wave-number spin wave scatters into a high wave-number excitation, create the possibility for additional nonlinear loss processes, often called decay instability processes. The time scale for these processes is on the order of the low power relaxation time. For YIG films, this time is in the range of

hundreds of nanoseconds. Such nonlinear decay processes can, in principle, play an important role in the formation of solitons from cw input signals, even though they are not important for the production of MME solitons from short input pulses with typical durations in the 10–20 ns range.

In order to examine the quantitative effects of nonlinear damping on soliton train formation in mode beating experiments, numerical modeling based on the one-dimensional nonlinear evolutional equation with linear and nonlinear damping terms has been performed. Note that, physically nonlinear damping terms come from the parametric processes, such as four wave decay and higher-order instabilities, which may occur simultaneously with modulational instability of the solitonic type. These parametric processes can contribute significantly to the total decay of the intense initial waves.[15]

The starting equation was the full torque equation of motion for the magnetization. It proves convenient to work with a reduced scalar complex response parameter u, defined through $u = m/2^{1/2}M_s$, where m is the root mean square (rms) transverse dynamic magnetization response. A series of transforms yields a working equation of the form

$$\frac{\partial u}{\partial t} + v_g \frac{\partial u}{\partial z} + \eta_0 u - i \left[\frac{D}{2} \frac{\partial^2 u}{\partial z^2} - (N - i\nu)|u|^2 u \right] = U(z,t).$$

$$(1)$$

This equation is a particular case of the Ginzburg-Landau equation,[16] previously studied, for example, in the context of solitons in nonlinear optics.[4] It also may be termed the one-dimensional nonlinear Schrödinger (NLS) equation with additional linear and nonlinear damping terms. The η_0, D, N, and ν parameters denote, respectively, the low power relaxation rate, the dispersion $\partial^2 \omega_k / \partial k^2$, the nonlinear response coefficient $\partial \omega_k / \partial |u|^2$, and the nonlinear damping. All indicated derivatives are evaluated at the appropriate (k, ω_k) operating point and at $|u| = 0$. The $U(z,t)$ term has a form similar to the time varying magnetic driving field $h(z,t)$ $= h_0(z) e^{i\omega_k t} (e^{i\Delta\omega t/2} + R e^{-i\Delta\omega t/2})$, where z is the propagation coordinate, $\omega = \pi(f_1 + f_2)$ is the average angular frequency, $\Delta\omega = 2\pi|f_1 - f_2|$ is the frequency separation, R is a relative amplitude control parameter, and t is time. It is important to note that this driving magnetic field is highly localized in space. It is defined by electric current, which is specified only in the narrow spatial zone where the input antenna is positioned. In other words, the right-hand term of Eq. (1) describes a localized excitation source.

For the analysis, Eq. (1) was Fourier transformed to yield a system of nonlinearly coupled first order differential equations for the spatial Fourier amplitudes of the dynamic magnetization. These equations were then solved numerically by the Runge-Kutta method. At each temporal step, the spatial MSBVW wave form profile was constructed from the computed Fourier spectrum by inverse fast Fourier transform techniques.

The calculations were done with D and v_g set to 1300 rad/cm^2 and -3.6×10^6 cm/s, respectively, based on the low power $\omega_k(k)$ dispersion curve data and MSBVW fits to these data. The low power relaxation rate η_0 was set to
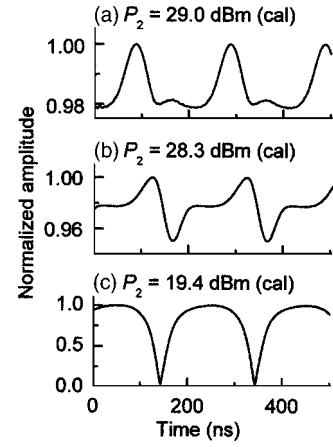

FIG. 2. Normalized amplitude versus time traces obtained from the numerical analysis for cw input signals at frequencies f_1 $= 5590$ MHz and $f_2 = 5595$ MHz. The input power P_1 was set at 19.4 dBm for all traces. The P_2 input powers were set as indicated for each graph. The "cal" denotes that these powers are calibrated values, based on a theoretical reduced input power $|u_{in}|^2$ vs input power P_{in} calibration of 7.7×10^{-5} mW^{-1}.

4.4×10^6 rad/s, based on direct probe measurements of the spatial decay of the low power MSW amplitude with cw input at one end of the film only. The N parameter was set at -1.1×10^{10} rad/s, based on the linear theoretical MSBVW $\omega_k(k)$ dispersion response, but with M_s replaced by $M_s(1 - |u|^2/2)$.[17] The nonlinear damping parameter ν was determined from a full analysis of the input power dependent output response for a single cw input signal following.[14] This analysis gave $\nu = 2 \times 10^9$ rad/s.

The computations were done for the experimental input frequencies f_1 and f_2. The input drive amplitudes controlled by h_0 and R were varied to give a range of corresponding input amplitudes u_1 and u_2 at $z = 0$. Output amplitude versus time profiles were obtained at various distances from the input point for different u_1 and u_2 amplitude combinations. These amplitudes were adjusted to give output profiles that mimicked the experimental responses as close as possible. As a quantitative point of contact with the experiment, the input $|u|^2$ values, taken as $|u_{in}|^2$, were also converted to the corresponding input power P_{in}, based on a full MSBVW microstrip transducer coupling analysis.[18] For the transducer and film parameters in the experiment, this $|u_{in}|^2/P_{in}$ conversion is 7.7×10^{-5} mW^{-1}.

Figure 2 shows representative results from the modeling for choices of the u_1 and u_2 input amplitudes that give a reasonable match to the experimental time traces in Fig. 1. The format is the same as for series (i) traces in Fig. 1, with all signals normalized to the peak values. The (a), (b), and (c) graphs were obtained for a common u_1 value of 0.082, and with u_2 set at 0.246, 0.227, and 0.082, respectively. From the $|u_{in}|^2/P_{in}$ calibration, these amplitudes correspond to P_1 $= 19.4$ dBm and P_2 values of 29.0, 28.3, and 19.4 dBm, respectively. The P_2 values are shown above their respective graphs. Note, in particular, that $P_2 > P_1$ for (a) and (b) and $P_1 = P_2$ for (c), with the same sequence as in Fig. 1.

The evolution of the time traces from (a), where u_1 and u_2 are unbalanced, to (c), where these input amplitudes are

equal, is strikingly similar to the results in Fig. 1. For (a), with $u_2 > u_1$ and $P_2 > P_1$, the nonlinear mode beating response is close to the bright soliton train signal in Fig. 1(a). For (c), with u_2 set equal to u_1, the computed trace almost perfectly reproduces the black soliton train in Fig. 1(c). While the match up in the time traces is impressive, one should also note that the corresponding input powers in two cases are approximately 4 dB too high, relative to the experiment. It is important to keep in mind that the calibration from the u values to power in dBm is purely theoretical, and the errors here could be substantial. The important point is that the inclusion of nonlinear damping can lead to dark solitons, as seen experimentally, even when such signals would not be formed based on the basic evolutional equation without damping.

In summary, this work reports on experimental observation of the simultaneous formation of temporal dark and bright soliton trains from a single magnetostatic carrier wave with attractive nonlinearity. The MSBVW dark and bright soliton trains were obtained from the induced modulational instability, which resulted from the mode beating of two cw signals at moderate power. The observed responses can be modeled from the Ginzburg-Landau equation. The qualitative agreement between the theoretical and measured traces indicates that nonlinear damping and decay instability considerations are the key to this type of spin wave soliton response.

[1] C. Sulem and P. L. Sulem, *The Nonlinear Schrödinger Equation* (Springer, New York, 1999).

[2] M. Remoissenet, *Waves Called Solitons: Concepts and Experiments* (Springer, Berlin, 1999).

[3] *Solitons in Action*, edited by K. Lonngren and A. Scott (Academic, New York, 1978).

[4] G. P. Agrawal, *Nonlinear Fiber Optics* (Academic, San Diego, 1995).

[5] B. A. Kalinikos, N. G. Kovshikov, and A. N. Slavin, Zh. Eksp. Teor. Fiz. **94**, 159 (1988) [Sov. Phys. JETP **67**, 303 (1988)].

[6] M. Chen, M. A. Tsankov, J. M. Nash, and C. E. Patton, Phys. Rev. Lett. **70**, 1707 (1993).

[7] R. Marcelli and P. De Gasperis, Appl. Phys. Lett. **65**, 249 (1994).

[8] H. Y. Zhang, P. Kabos, H. Xia, R. A. Staudinger, P. A. Kolodin, and C. E. Patton, J. Appl. Phys. **84**, 3776 (1998).

[9] C. S. Tsai, D. Young, and S. A. Nikitov, J. Appl. Phys. **84**, 1670 (1998).

[10] G. A. Melkov, Yu. V. Kobljanskyj, A. A. Serga, V. S. Tiberkevich, and A. N. Slavin, J. Appl. Phys. **89**, 6689 (2001).

[11] H. Benner, B. A. Kalinikos, N. G. Kovshikov, and M. P. Kostylev, Pis'ma Zh. Eksp. Teor. Fiz. **72**, 306 (2000) [JETP Lett. **72**, 213 (2000)].

[12] A. N. Slavin and I. V. Rozhdestvenski, IEEE Trans. Magn. **30**, 37 (1994).

[13] M. M. Scott, Ph.D. thesis, Colorado State University, 2002.

[14] V. S. L'vov, *Wave Turbulence Under Parametric Excitation* (Springer, Berlin, 1994).

[15] M. M. Scott, C. E. Patton, M. P. Kostylev, and B. A. Kalinikos, J. Appl. Phys. **95**, 6294 (2004).

[16] I. S. Aranson and L. Kramer, Rev. Mod. Phys. **74**, 99 (2002).

[17] *Spin-Wave Envelope Solitons in Magnetic Films*, edited by P. E. Wigen (World Scientific, Singapore, 1994), Chap. 9.

[18] D. D. Stancil, *Theory of Magnetostatic Waves* (Springer, New York, 1993).